

## A NOVEL FORM OF DAMPER FOR TURBO-MACHINERY

R.D. Brown and J.A. Hart  
Heriot-Watt University  
Riccarton, Edinburgh EH14 4AS  
Scotland

Anti-swirl vanes are used by some manufacturers to delay the full development of half speed circulation in annular clearance spaces. The objective is to reduce the aerodynamic cross-coupling in the forward direction. The novel feature of a jet damper is a number of tangential nozzles discharging against the rotor surface speed. Some preliminary results on a 33.9 Kg rotor demonstrate that significant reductions in amplitude are obtained at the synchronous critical speeds.

## INTRODUCTION

The vibration of rotating machinery is due to a large number of forces which act on the surface of a rotating shaft. These forces include mechanical unbalance, bearing forces and fluid forces from impellers, seals, diffusers and labyrinths among others. If the response to the net action of all these forces is excessive the result is an unacceptable machine. An increase in damping of the rotor system can reduce the vibration response to acceptable levels.

Some experimental work on a small scale test rig has demonstrated that high speed tangential flow acting on the surface of a rotor can produce significant cross-coupling forces. If the direction of the flow is against the surface velocity then additional forces acting against rotor motion can be produced. These forces will considerably reduce response to synchronous unbalance and may also combat forward sub-synchronous whirl. A major advantage is that these forces act in the same direction as external damping but do not depend significantly on rotor motion.

An experimental test rig has been constructed to demonstrate the feasibility of the jet damper concept to reduce synchronous and sub-synchronous whirls in the forward direction. The rig has been designed to explore the effects of jet velocity and surface roughness on the magnitude of the force produced. The aim of the experimental work is to produce design data for a damper on a full size machine.

Among the potential advantages of a jet damper are the ease of fitting to existing machines, using a shaft extension if necessary. If such a damper is installed it can be left in an un-operational state until required. For example run-down or the detection of sub-synchronous vibration. Tangential flow on the rotor surface can then be initiated using a fast acting solenoid or fluidic valve. Damping forces can then be introduced as and when required.

## NOMENCLATURE

C	radial clearance	h	local radial clearance
H	total head	n	eccentricity ratio
L	length	$\bar{u}$	mean fluid circumferential velocity
P	static pressure	u	local fluid circumferential velocity
R	radius	Re	Reynolds Number
$F_x, F_y$	fluid forces	$\theta$	peripheral angle, measured from minimum gap
$K_{xx}, K_{yy}$	direct stiffness coefficients	$\rho$	density
$K_{xy}, K_{yx}$	cross stiffness coefficients	$\delta$	rotor displacement
$\bar{K}_{xx}, \bar{K}_{yy}$	non-dimensional direct stiffness coefficient	$\tau_0$	wall shear stress
$\bar{K}_{xy}, \bar{K}_{yx}$	non-dimensional cross stiffness coefficient	$\omega$	angular velocity
f	friction coefficient	$\nu$	Kinematic viscosity

## BACKGROUND

Significant vibration response in rotating machines is either forced response or instability. Both types of response can be reduced by external damping.

### Forced Response

Response is largely a matter of unbalance distribution especially where flexible rotors are involved. In certain cases a rotor that was initially well balanced may have been running for a long time at a running speed considerably above a natural frequency. The original balance is often disturbed by a combination of blade erosion and deposits from the process fluid. For large machines not fitted with a braking mechanism the run down time is considerable thus allowing a significant time at speeds near resonance. This problem is recognised in the petro-chemical industry by specifying that vibration measurements are obtained during run-down tests. High response is due to the small damping of the natural frequencies of the rotor system. One well known method of reducing vibration response is to increase damping. However conventional methods of damping rely on using the motion of the vibrating body itself to provide the damping force e.g. an oil dash pot or shock absorber. As the motion is necessarily small, viscous fluids are normally used to provide sufficient damping forces. For rotating machinery squeeze film bearings are often used particularly in aero engines.

### Instability

A common problem found in high speed turbo-machinery rotors is instability due to increases of speed and/or load beyond the stability boundary. The problem usually manifests itself as an increase in the vibration level at a non-synchronous frequency. In most cases this frequency is a natural frequency of the system which

is insufficiently damped. As this frequency is often exceeded in the acceleration to running speed its reappearance as a result of instability is normally sub-synchronous i.e. at a frequency less than that corresponding to running speed. However unlike synchronous resonance it is usually impossible to pass through successfully without either reduced load or speed.

Instabilities of this sort are generally referred to as aerodynamic cross-coupling. A simple form of cross-coupling can be modelled by a lateral motion of the shaft causing a force perpendicular to that displacement. When the force vector is aligned with the translational velocity of the precessing shaft it behaves as a negative damping force. Experimental measurements of cross-coupling forces of this general nature are well established in bearings, impellers, blade rings and seal passages. In small annular clearances, typical of labyrinth seals the inlet flow, mainly axial, develops a strong circumferential component as a result of friction from the rotating shaft. Eventually the mean tangential component is equivalent to half the surface velocity of the shaft. Following a suggestion in reference 1 some manufacturers fit anti-swirl vanes at the entrance to labyrinth seals to impose a backward swirl to the inlet flow. This delays the full development of the mean circumferential half-speed swirl and so reduces any cross-coupling that may be present in the labyrinth. A combination of a roughened stator with a smooth rotor has been shown in reference 2 to reduce the mean tangential velocity. However neither of these approaches essentially alters the basic nature of the circumferential flow.

### **Principle of Damper**

The damper uses high velocity backward facing jets impinging tangentially on a roughened rotor surface which can produce significant increases in damping forces and substantially improve stability characteristics of turbo-machines. The essential feature of the jet damper is to use a number of high speed jets of fluid to give a relative motion in the appropriate direction to provide a damping force. As the relative velocity is largely independent of shaft orbital motion, high velocities can be used and therefore low viscosity fluids e.g. air are practical to generate forces of considerable magnitude.

### **PRELIMINARY RESULTS OBTAINED USING A PROPRIETARY ROTOR KIT**

A proprietary rotor kit was adapted by the manufacture of a chamber and nozzle assembly to provide an annular space around which fluid could be circulated at high velocity. The rotor consisted of a 280 mm. long shaft of 9.5 mm. diameter, with an 0.846 Kg. steel disc of diameter 76.2 mm. mounted at midspan. This disc was supplied with its surface ground to give a smooth finish. Supporting the shaft at either end were brass bushes mounted in housings with a single rubber 'O' ring between the bush and housing. The rotor was driven by a 380 W reversible d.c. electric motor connected to the shaft through a flexible coupling. On running the rotor it was found that the first critical speed was at 3150 r.p.m. (52.5 Hz.), thus the maximum motor speed of 7000 r.p.m. meant that rotor speeds above twice the first critical could be achieved. More details are discussed in reference 3.

### **Plenum Chamber and Nozzle Assembly**

An exploded view of the chamber and nozzle assembly is shown in figure 1. This was constructed from three aluminium plates arranged in a sandwich assembly, forming

a chamber into which a compressed air supply could be fed. Mounted on one plate were four nozzles of 10 degrees included angle and 0.50 mm. by 9.50 mm. exit area. These nozzles directed high velocity air tangentially onto the surface of the central mass. Radial clearance between the stator and the rotor was 0.46 mm.

A pair of non-contact proximity probes, placed 90 degrees apart, measured the shaft vibration at a location approximately midway between the central mass and a bearing. The output from these probes was fed into an X-Y oscilloscope and a real-time spectrum analyser which derived the frequency components of the vibration.

### Test Procedure and Results

The tests conducted can be classified into two main groups

#### (a) Effect of Fluid Flow on Rotor Stability

While running the rotor at constant speed, the plenum pressure was carefully increased and both the resultant orbit and response spectrum noted. Any instability could then be observed from the orbital pattern and the plenum pressure at the onset of this instability recorded. This test was repeated for flow in the same (forward) and opposite (reverse) direction to shaft rotation, and for a number of rotor speeds.

It was found that an instability could be induced by the circumferential flow of air in the annulus. The pressure ratio (plenum pressure/atmospheric pressure) at the onset of this instability is plotted against the speed ratio (rotor speed/first critical speed) on figure 2. It can be seen that the stability boundary appears to be unaffected by the direction of rotor rotation. However it should be noted that the nozzle exit velocity is of the order of 100 - 250 m/s compared with a maximum rotor surface speed of only 25 m/s. The destabilising forces generated are therefore of similar magnitude regardless of the direction of rotation. This test was found to be highly repeatable, the variation in the required pressure ratio being about 3%.

#### (b) Effect of Fluid Flow on Rotor Response

The averaging facilities of the spectrum analyser were used to obtain smoothed spectral densities of the rotor response for constant speed tests at various values of plenum pressure. This was repeated for a number of rotor speeds in both the forward and reverse direction.

A typical set of frequency spectra for the rotor response are shown on figure 3. Similar data was first shown in reference 4. These show the response for various running speeds at a steady plenum gauge pressure of 41.37 kN/m<sup>2</sup> (6.0 psig). This pressure corresponds to a nozzle exit velocity of about 230 m/s. As a threshold speed is reached sub-synchronous vibration suddenly appears the frequency of which was found to be about 50.4 Hz. This frequency is slightly less than the system resonant frequency of 52.5 Hz. A typical orbit is also shown once sub-synchronous behaviour is initiated for both forward and reverse flow.

While performing the experimental work it was observed that if rotation was in the opposite direction to the high velocity fluid flow, then any value of plenum pressure tended to reduce the amplitude of the synchronous vibration. This reduction was pronounced at speeds near the first critical speed.

As a result of this preliminary experimental work it was concluded that the use of reverse flow as a means of reducing synchronous vibration amplitudes in the speed range around the first critical was an effect worthy of further investigation. It should be noted that these results were obtained using nominal values of radial clearance and a smooth rotor surface. Variation in these parameters could lead to experimental data for the optimal design of an industrial device.

### **EXPERIMENTAL TEST RIG**

The main objective of the more elaborate test rig was to isolate the circumferential velocity induced effects from other rotordynamic phenomena. As this work is concerned with the damping of supercritical rotors, the maximum rotor speed must lie well above its first critical. Further requirements of the rig were a realistic rotor velocity and ease of disassembly and modification.

The experimental approach being undertaken is to measure the effect of the fluid flow on the vibration response of the rotor for a number different values of annular chamber geometry and rotor surface roughness. Measurements are planned under various fluid supply pressures.

### **Overall Layout**

The test rig consists of a vertical flexible shaft onto which a central disc is mounted, surrounded by a nozzle chamber. Into this chamber, pressurised fluid is fed before being injected tangentially onto the disc surface by virtue of the nozzle arrangement.

Consistent with the need to isolate other rotordynamic phenomena, the rotor is mounted vertically in self aligning ball bearings thus eliminating gravitational and oil-film effects respectively. These grease lubricated bearings allow for the angular misalignment caused by vibration of the flexible shaft.

### **Component Design**

The rotor was constructed from a machined steel shaft of about 45 mm. diameter onto which three discs were shrunk. A central steel mass 152 mm. long and 149 mm. in diameter, provided a rotor surface velocity of up to 80 m/s at the maximum rotor speed. In order to avoid any problems due to an internal friction mechanism at the shrink fit interface, the shaft was undercut so that the contact was only over two 38 mm. lengths. Two brass discs 38 mm. wide and 123 mm. in diameter were similarly attached to the shaft at about one quarter and three-quarters span. These discs performed two basic functions. They provided a surface, free from residual magnetic impurities, from which the rotor deflection could be measured using a pair of non-contact proximity probes. Secondly, these discs acted as a safety device such that if excessive rotor deflection occurred then the disc would come into contact with a PVC guard ring before damage was done to the nozzle assembly by the central rotor mass. Following fabrication, the complete rotor assembly, of mass 33.9 kg, was finished ground to obtain the required surface finish and concentricity tolerances between the discs and bearing journals. Tapped holes were machined in the end faces of the central disc into which grubscrews could be inserted in order to partially balance the rotor. A known amount of unbalance could then be supplied in order to investigate the unbalance response of the rotor.

At the design stage the rotor was modelled using a computer program available within

the department. This program calculates the critical speeds, mode shapes and forced response using a transfer matrix/Rayleigh-Ritz method. This software is described in more detail in reference 5. Utilising this program the rotor was designed to have a first critical speed of about 4200 r.p.m.

Drive was by means of a horizontally mounted 8.5 kW variable speed reversible DC motor with the motor output shaft being connected to a right angle gearbox of ratio 1.1 through a flexible coupling. Using a timing belt and toothed pulleys of ratio 1:3.33, a maximum rotor speed of 8000 r.p.m. could be achieved.

The rotor was mounted in a casing consisting of three main sections - the upper and lower body and a central chamber which housed the nozzle assembly. These components were fabricated from steel tube onto which flanges were welded. To ensure concentricity throughout the assembly, each body had spigots machined thus ensuring a total eccentricity of not greater than 0.025 mm. The upper and lower bodies were press fitted with steel rings which acted as mounts for the PVC guard rings. The upper bearing housing was bolted to the upper body and the lower housing to a plate which was mounted between the lower body and the base. A sectioned assembly of the main body of the test rig is shown on figure 4.

Compressed air was chosen as the working fluid being supplied to the test rig from the departmental compressors via a receiver, filter and regulating valve. Four delivery pipes supplied the fluid to the plenum chamber which allowed a settled pressure to be achieved before entry to the nozzle assembly. Machined aluminium blocks were arranged to create eight convergent nozzles of about 10 degrees included angle. The nozzle block geometry and a section through the assembly are shown in figure 5. These blocks were assembled in six layers of eight blocks each block being located by a spring dowel pin into its neighbour. Steel rings top and bottom of the stack allowed eight through bolts to fasten the assembly. The exit dimensions of each nozzle formed by the build up of six blocks was 0.51 mm. by 127 mm. with the geometry being such that the flow was tangential to the rotor surface. The flow discharged through four ports in the wall of the upper and lower bodies. Figure 6 shows the built up nozzle assembly.

### **Experimental Parameters, Procedure and Instrumentation**

The experimental parameters are:

- (i) Rotor speed
- (ii) Plenum pressure and mass flowrate
- (iii) Radial clearance between nozzles and rotor
- (iv) Rotor surface roughness
- (v) Unbalance

For each setting of these parameters the rotor response is measured at the upper and lower brass discs.

Rotor speed was measured by a proximity probe mounted in the upper bearing cover plate. A small slot cut in a disc mounted on the shaft end provided a once per revolution signal for an electronic counter. Plenum pressure was measured at eight locations equi-spaced around the chamber using diaphragm type pressure transducers. These tappings provided information regarding any assymetry in the plenum circumferential pressure field. The fluid mass flowrate through the rig was measured by a commercially available flow sensor. Mounted on the main supply line to the

rig downstream of the regulating valve, this consisted of a device which measures the difference between the mean dynamic and static pressure in the line. Measurement of this difference and the flow temperature allowed the flowrate to be calculated by reference to the flow instrument manual. Further experimental values recorded included the plenum temperature and the rig outlet pressure and temperature. A pressure tapping was also made through the nozzle assembly and into the annular space such that the pressure at the exit from a nozzle could be recorded. A close up of the main body of the test rig is shown in figure 7.

Whereas the tests regarding the effect of fluid flow parameters on the rotor response can be carried out without any modification of the test rig, the variation in the radial clearance and the rotor surface roughness require stripdown and reassembly. These two parameters can be altered by means of steel sleeves which are machined to fit over the central rotor mass, secured with setscrews. The external diameter and machining of these sleeves dictates the radial clearance and surface roughness employed.

During a typical test run, analysis of the signals generated by the four proximity probes is carried out using a real-time spectrum analyser. Averaging and decomposition of the time histories into frequency spectra can then be carried out while a test is proceeding. On completion of a test, averaged time histories and frequency spectra are transferred to a disc file via an IEEE interface unit controlled by a microcomputer. Supplementary data such as the plenum pressure field, temperatures and flowrate data can be added to this file via the computer keyboard. Data analysis, hardcopy output and graphical presentation can then be carried out as required. A schematic diagram of the complete test rig and instrumentation is shown on figure 8 while figure 9 illustrates the complete experimental set up and data logging equipment.

On running the rotor a casing resonance which lay within the speed range was observed, thus necessitating the fabrication of four angled struts which stiffened the rotor casing. With this modification in place the first critical speed was raised to about 5000 r.p.m. due to the increased support stiffness. Two critical speed close to one another were observed due to a slight anisotropy of the casing and supporting frame stiffness. The structural resonance was not completely eliminated however the vibration amplitudes produced were considerably reduced.

## EXPERIMENTAL RESULTS

All experimental measurements of response presented in figures 10 - 12 are obtained by ensemble averaging of 256 time records from which time averaged orbits can be plotted.

Figure 10 and figure 11 show the response at the upper brass disc for a combination of reverse flow, a smooth rotor surface and a radial clearance of 0.508 mm. The two plots shown represent the orbits of significant magnitude in the speed range thus corresponding to the two critical speeds. The outer orbits are obtained with no flow present whereas the smaller time averaged orbits are obtained as a result of reverse flow being present. Each successive orbit represents a pressure increase of  $6.98 \text{ kN/m}^2$  (1.0 psi.) in the plenum chamber.

It is obvious that a distinct reduction in the response at these two speeds is obtained by the introduction of reverse flow in the annular space around the rotor. A plenum gauge pressure of  $34.5 \text{ kN/m}^2$  (5.0 psig.) can be seen to reduce the response

by over 50%. This pressure corresponds to a mean air velocity at nozzle exit of around 70 m/s compared with a rotor surface speed of about 40 m/s. This velocity is calculated from the plenum pressure and temperature and a single static pressure measurement near a nozzle exit.

The orientation of the elliptical orbit can be seen to change as the pressure increases as would be expected by the introduction of a transverse force acting on the rotor. These orbits result from residual unbalance only and thus this change in orientation cannot be directly compared to conventional phase angle.

The effect of reverse flow on rotor response was measured for a number of rotor speeds in the region of resonance and some results are shown on figure 12. Each point on this graph represents a stable orbit with no significant non-synchronous components visible on the frequency spectra.

Not only are the magnitude of the two peaks corresponding to the critical speeds reduced, but a considerable reduction is evident across the speed range. As the vibrational amplitudes in the region of resonance are controlled by the amount of damping present, it would appear that reverse flow has dramatically increased the system damping. Both synchronous peaks appear to be shifted to a higher frequency as would be predicted by a single degree of freedom model with increased damping. A reduction in the system natural frequency might be expected due to the negative stiffening of the Bernoulli Effect (See Appendix A). However the experimental results would suggest that the increased damping dominates this movement of the peaks.

The above results show that a reverse flow of relatively low velocity considerably reduces the synchronous response of the rotor. The effect of surface roughness and radial clearance may lead to even greater reductions being possible. Results to date illustrate that reverse flow may be a feasible and reliable basis for the development of a damper to be used on industrial turbomachinery.

### JET DAMPER DESIGN

The concept of a jet damper has been shown to work on a laboratory scale. However it is necessary to demonstrate that it is practical for a full size machine. If we consider a compressor of about 90 Kg. mass and a natural frequency of 80 Hz. then the shaft stiffness is around  $23 \times 10^6$  N/m.

Assuming the following data for a jet damper:

R = 70mm  
L = 50 mm  
 $\rho$  = 1.22 Kg/m<sup>3</sup>  
 $\bar{u}$  = 150 m/sec  
C = 0.5 mm

then:  $\frac{RL \rho \bar{u}^2}{2C} = 96000$  N/m

Therefore the direct stiffness coefficient (see Appendix A) is about 600,000 N/m which is 2.5% of the shaft stiffness.

The magnitude of the cross-stiffness depends on the value of the friction coefficient  $f$ . For the assumed conditions the Reynolds number based on mean flow  $\bar{u}$  is 5100.

In this region the friction depends on the roughness and the majority of the data available is only concerned with smooth or moderately rough surfaces. If the surface is deliberately roughened then  $f$  could lie between 0.01 and 0.1. In this case the cross stiffness could be as large as 60,000 N/m. This is a significant fraction of the cross-stiffness magnitude associated with impeller and diffuser instability. Hence two or three dampers of these dimensions suitably located could act against forward whirl and so increase the stability margin.

If the friction force is too large (a combination of a number of damper jets with high velocity) there is a danger of promoting a backward whirl as discussed above. An arrangement which incorporates a degree of semi-active control would be necessary. A prime requirement would be fast acting valves controlling the nozzle flow. However this would be alleviated if the essential repetitive nature of the rotor motion was taken into account.

## APPENDIX A

### STIFFNESS COEFFICIENTS

The basic purpose of a number of tangential jets is to obtain a high circumferential flow acting against the forward rotation of the rotor. A simplified analysis assumes a constant circumferential flow in an annular channel at the periphery of a spinning rotor, figure 13. When the rotor is concentric with the stator the fluid friction is a pure torque due the mean flow  $u$  in the radial clearance  $C$ . However when the rotor is moved laterally the overall effect of the friction force acts at right angles to the displacement. When the direction of the jets is against the forward rotor motion the friction force acts against forward precession thus giving extra damping.

#### Direct Stiffness

With regard to Figure 13 a displacement  $\delta$  in the positive  $x$  direction produces a normal pressure distribution on the rotor surface which can be obtained using Bernoulli.

$$P + \frac{1}{2} \rho u^2 = H$$

Resolving pressures:

$$F_x = -RL \int_0^{2\pi} (H - \frac{1}{2} \rho u^2) \cos \theta d\theta, \quad F_y = -RL \int_0^{2\pi} (H - \frac{1}{2} \rho u^2) \sin \theta d\theta$$

Since  $h = C(1 - n \cos \theta)$ ,  $n = \delta/c$  and letting  $u = \bar{u} C/h$

then by substitution and neglecting  $n^2$  and higher powers:

$$F_x = RL \rho u^2 \pi n \quad \text{and} \quad F_y = 0$$

Therefore direct stiffness coefficient  $K_{xx} = F_x/\delta = RL\pi u^2 \rho/C$

Defining non-dimensional stiffness  $\bar{K}_{xx} = \frac{CK_{xx}}{\frac{1}{2} \rho u^2 RL}$

then  $\bar{K}_{xx} = -2\pi$

## Cross Stiffness

Referring to figure 13 for a displacement  $\delta$  in the positive x direction the friction forces  $F_x$  and  $F_y$  are obtained by integrating the shear stress components round the rotor surface.

$$F_x = RL \int_0^{2\pi} \tau_0 \sin\theta \, d\theta \qquad F_y = -RL \int_0^{2\pi} \tau_0 \cos\theta \, d\theta$$

Now  $\tau_0 = \frac{1}{2}\rho u^2 f$  where  $f = 0.079R_e^{-0.25}$  assuming fully developed turbulent flow.

Reynolds Number  $R_e = \bar{u}C/\nu$  or  $uh/\nu$  locally

Now this particular friction coefficient is appropriate for smooth pipes in well developed turbulence. Friction relationships for rough sections of shaft in annular clearances will obviously need to be determined experimentally.

As before by substitution and neglecting  $n^2$  and higher powers

$$F_x = 0 \quad , \quad F_y = -RL \rho \bar{u}^2 f \pi n$$

Since  $K_{yx} = -F_y/\delta$  then  $K_{yx} = RL \rho \bar{u}^2 \pi/C$

Defining non-dimensional stiffness  $\bar{K}_{yx} = \frac{CK_{yx}}{\frac{1}{2}\rho\bar{u}^2RL}$

$$\text{then } \bar{K}_{yx} = 2\pi f$$

Following a similar analysis for a rotor displacement in the y direction the fluid forces can be summarised as

$$\begin{bmatrix} F_x \\ F_y \end{bmatrix} = \frac{\rho\bar{u}^2RL\pi}{C} \begin{bmatrix} 1 & f \\ -f & 1 \end{bmatrix} \begin{bmatrix} x \\ y \end{bmatrix}$$

## APPENDIX B

### ADDITIONAL MATERIAL PRESENTED AT WORKSHOP

The effect of reverse flow on response was further investigated by conducting run-down tests on the rotor. Figure 14 presents waterfall diagrams of a typical run-down for the cases of no flow and reverse flow caused by a plenum pressure of 41.4kN/m<sup>2</sup>. It can be seen that a large reduction in the synchronous amplitude is obtained as a result of the reverse flow. These waterfall diagrams also show that no significant non-synchronous vibration components are present. The magnitudes of the synchronous components are plotted on figure 15 for each orthogonal direction.

The results generated by these run-down tests again illustrate that a damper based on reverse flow may indeed be a feasible means of reducing synchronous

vibration amplitudes. The use of such a device during run-up or run-down through critical speeds is also clearly shown.

As a matter of interest, tests were conducted to investigate the effect of flow in the same direction as rotation on the response. Figure 16 displays the effect of a plenum pressure of  $34.5\text{kN/m}^2$  on the synchronous amplitude at a number of steady rotor speeds. It can be seen that while the response is slightly suppressed at the first peak, it is magnified at the second peak. There is also a shift to a higher frequency of both peaks. Figures 17 and 18 show the frequency response and synchronous amplitude during run-down. A small sub-synchronous component of unknown origin can be seen in the response. The overall effect of forward flow is obviously detrimental to the response of the rotor.

### REFERENCES

1. Black, H.F.; Allaire, P.E. and Barrett, L.E.: Inlet Flow Swirl in Short Turbulent Annular Seal Dynamics. 9th International Conference in Fluid Sealing, BHRA Fluids Engineering, Leeuwenhorst, The Netherlands, April 1981.
2. Von Pragenau, G.L.: Damping Seals for Turbomachinery. NASA Technical Paper 1987, 1982
3. Hart, J.A. and Brown, R.D.: Laboratory Demonstration of Sub-Synchronous Rotor Vibration Induced by Fluid Friction. Paper accepted for publication International Journal of Mechanical Engineering Education.
4. Leong, Y.M.M.S. and Brown, R.D.: Experimental Investigations of Lateral Forces Induced by Flow through Model Labyrinth Glands. Proceedings 3rd Workshop on "Rotordynamic Instability Problems in High-Performance Turbomachinery". NASA CP 2338, May 1984.
5. Black, H.F.: Calculation of Forced Whirling and Stability of Centrifugal Pump Rotor Systems. Journal of Engineering for Industry, Trans. of the ASME. Paper No. 73-DET-131.
6. Brown, R.D.: Improvements in or relating to Dampening the Radial Vibration of Rotors. U.K. Patent Application, Patent Application No. 8421142, August 1984.

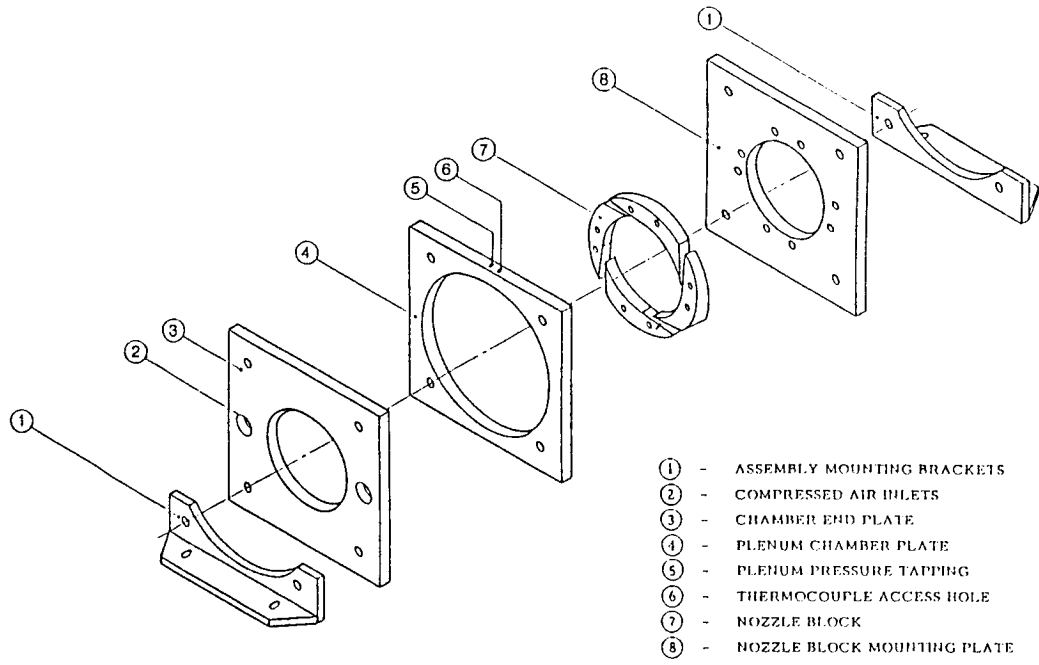


Figure 1 Chamber and nozzle assembly

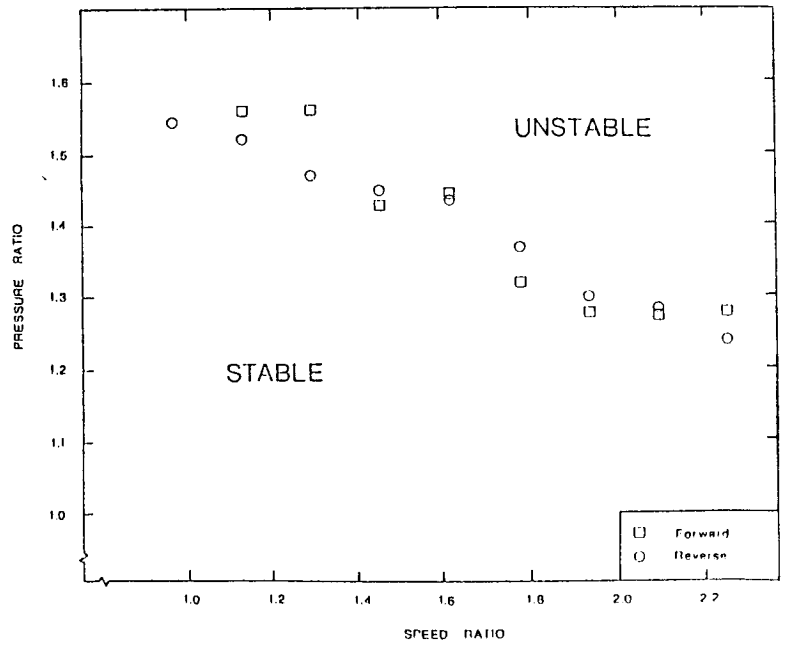


Figure 2 Rotor stability boundary

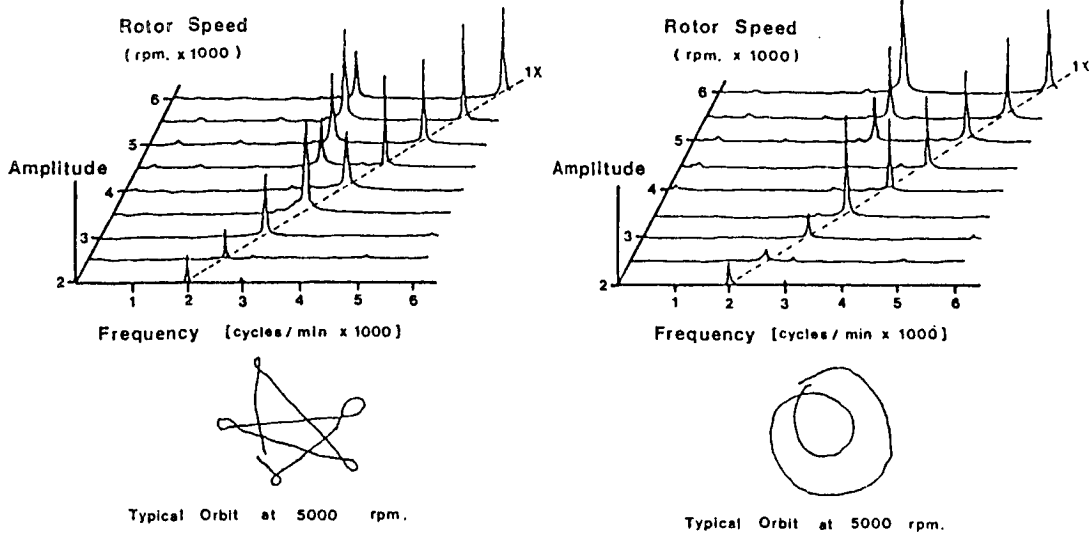


Figure 3 Response and orbit plots

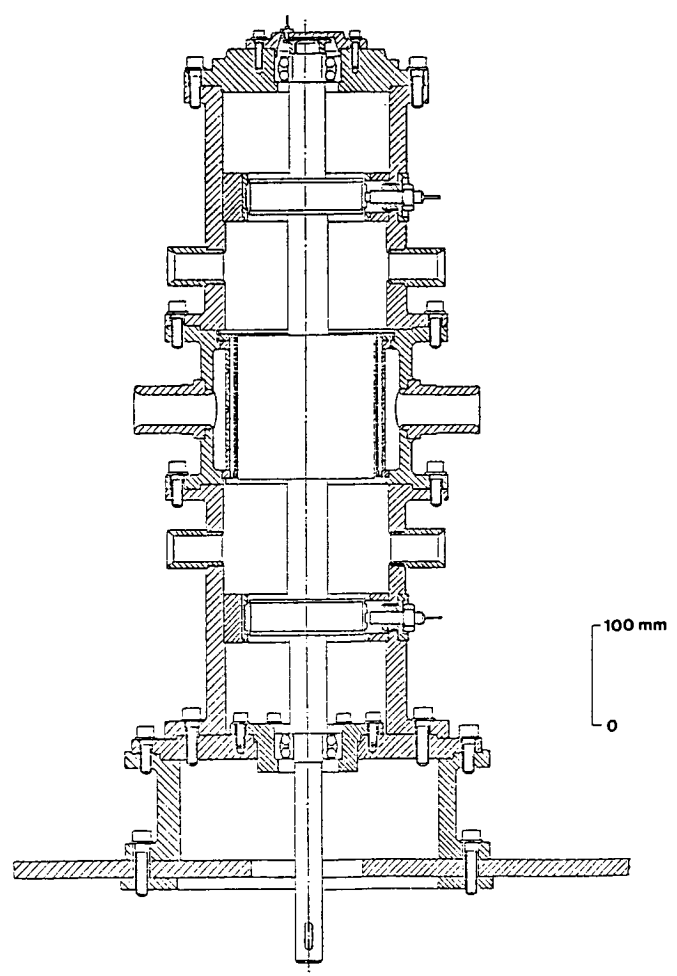


Figure 4 Sectioned assembly of test rig (main body)

ORIGINAL PAGE IS  
OF POOR QUALITY

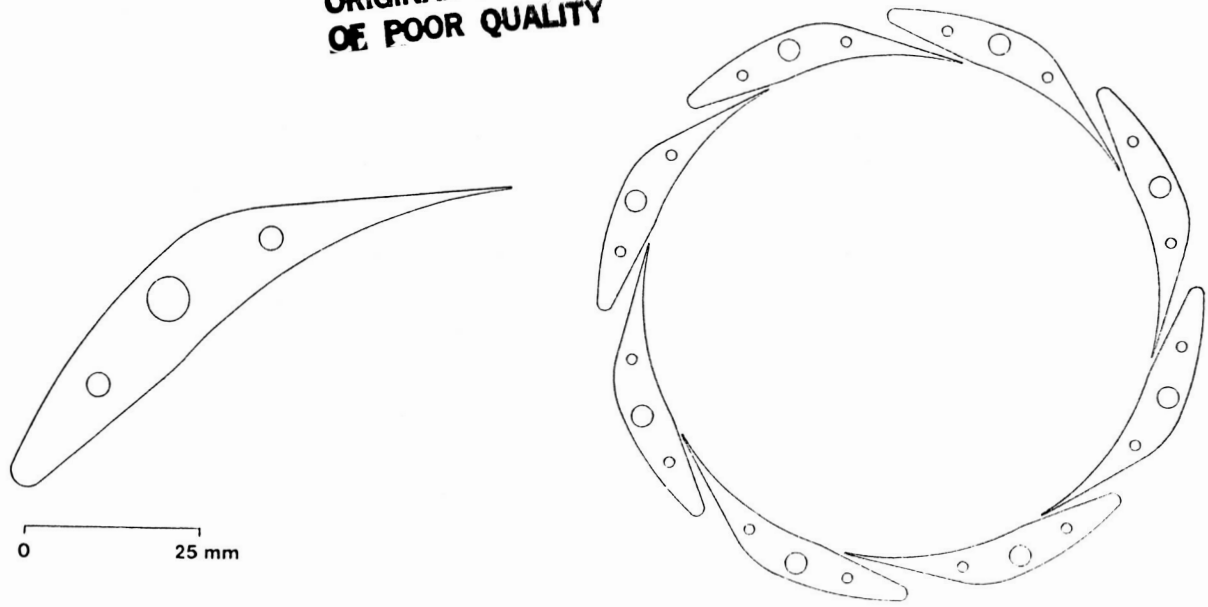


Figure 5 Nozzle block geometry and section through assembly

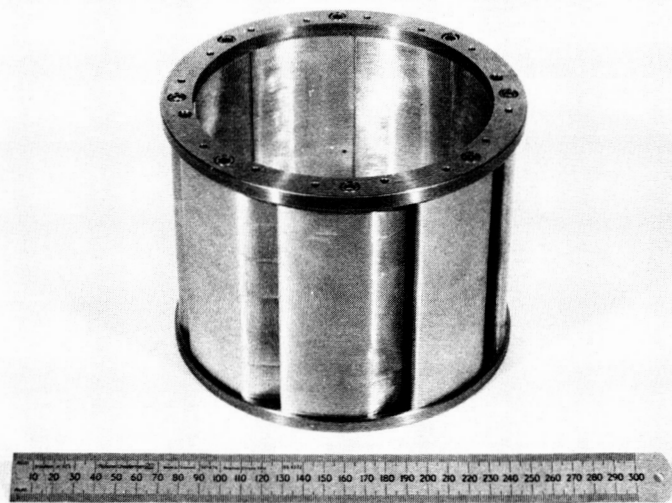


Figure 6 Built up nozzle assembly



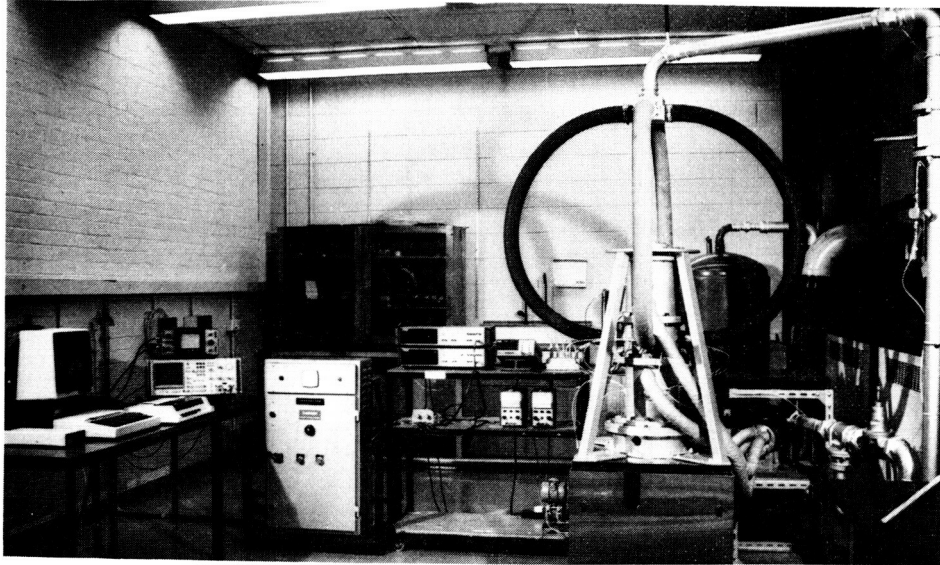


Figure 9 Experimental set-up

ORIGINAL PAGE IS  
 OF POOR QUALITY

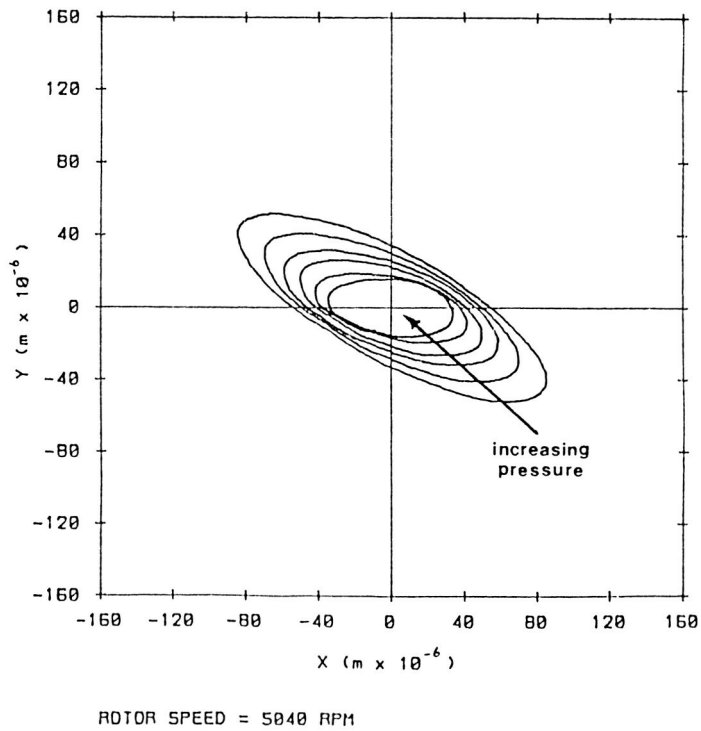
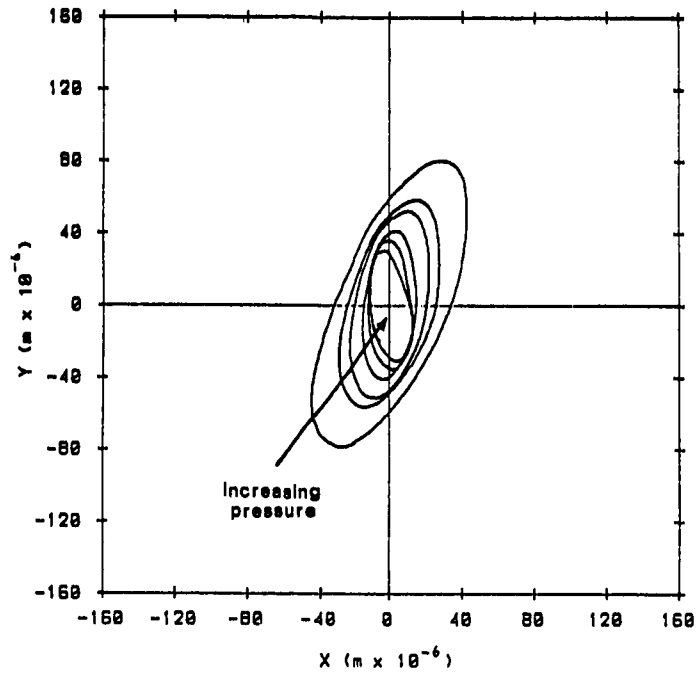


Figure 10 Effect of reverse flow on orbit  
 at 5040 r.p.m.



ROTOR SPEED = 5400 RPM

Figure 11 Effect of reverse flow on orbit at 5400 r.p.m.

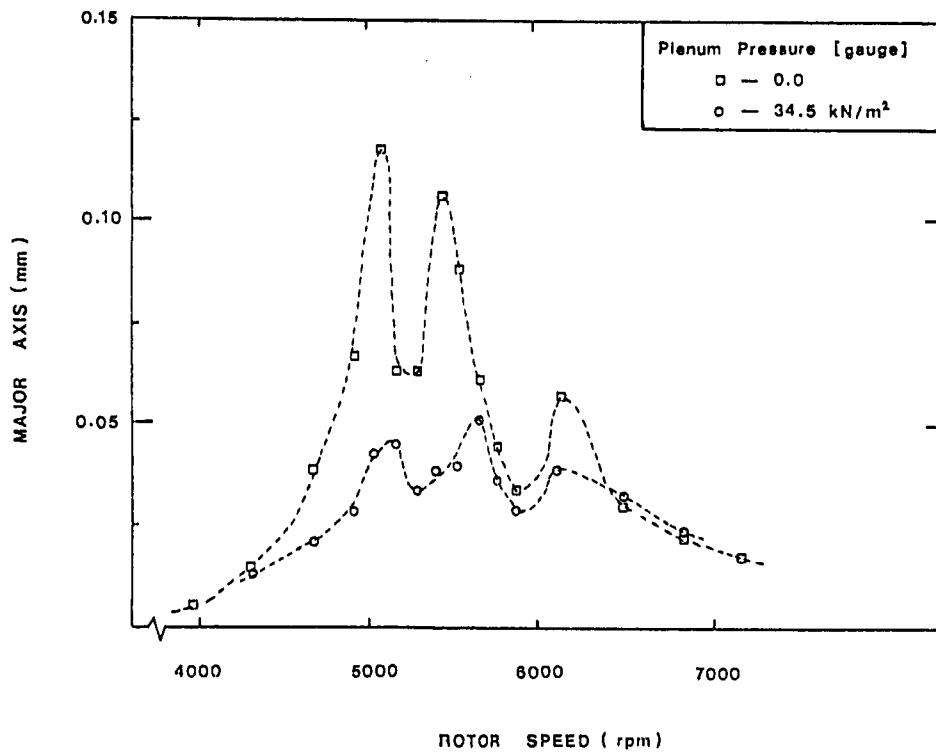


Figure 12 Rotor unbalance response, effect of reverse flow

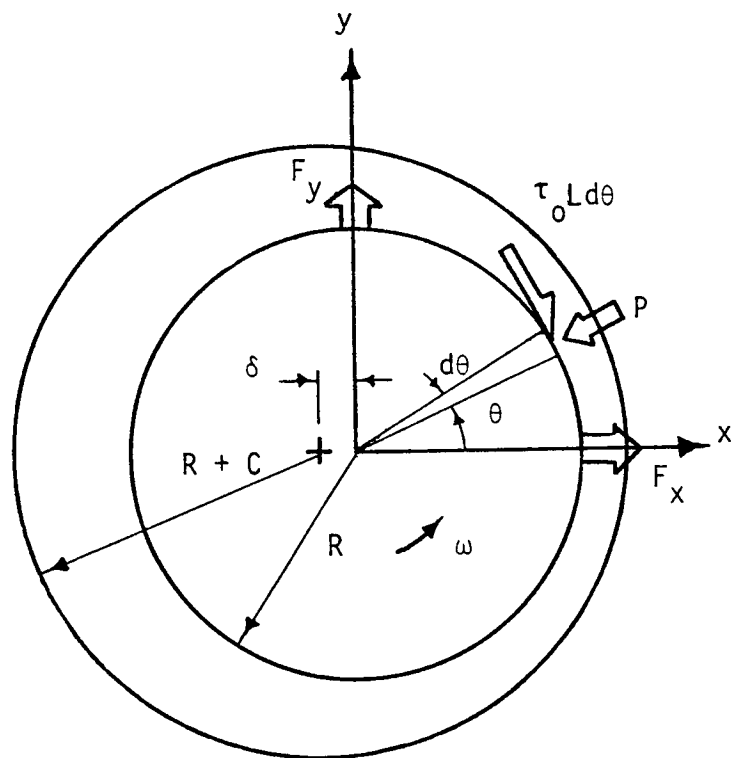


Figure 13 Annular gap geometry

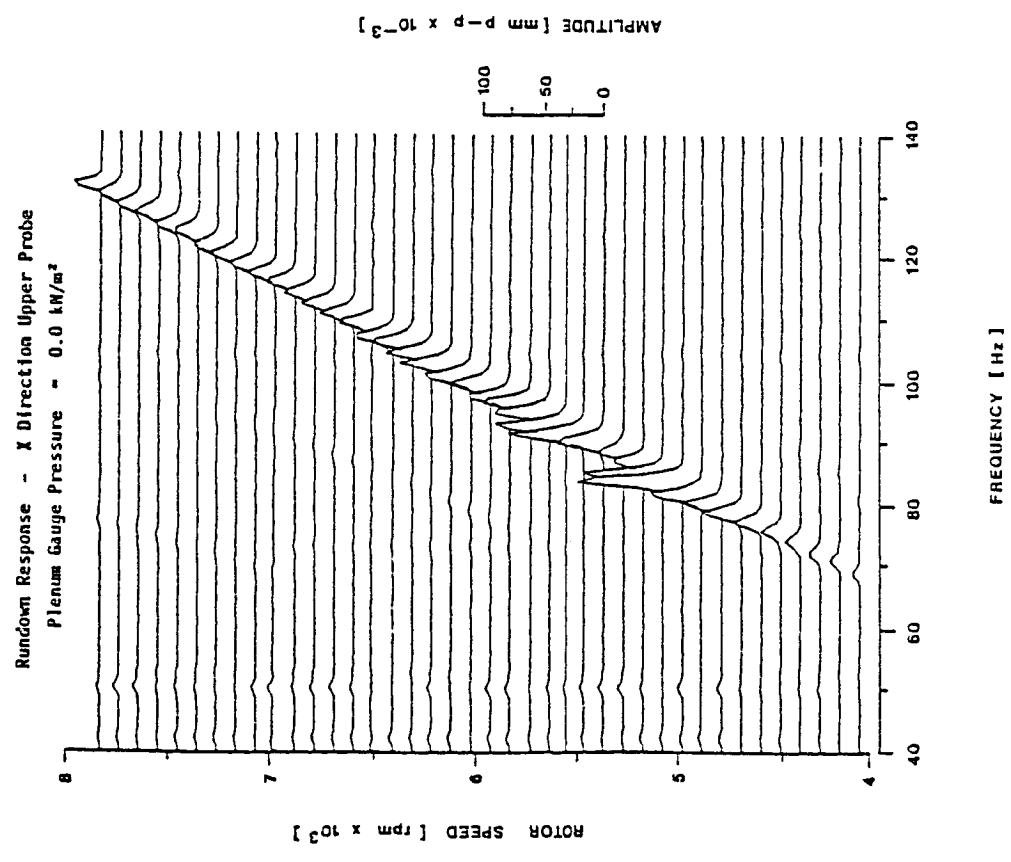
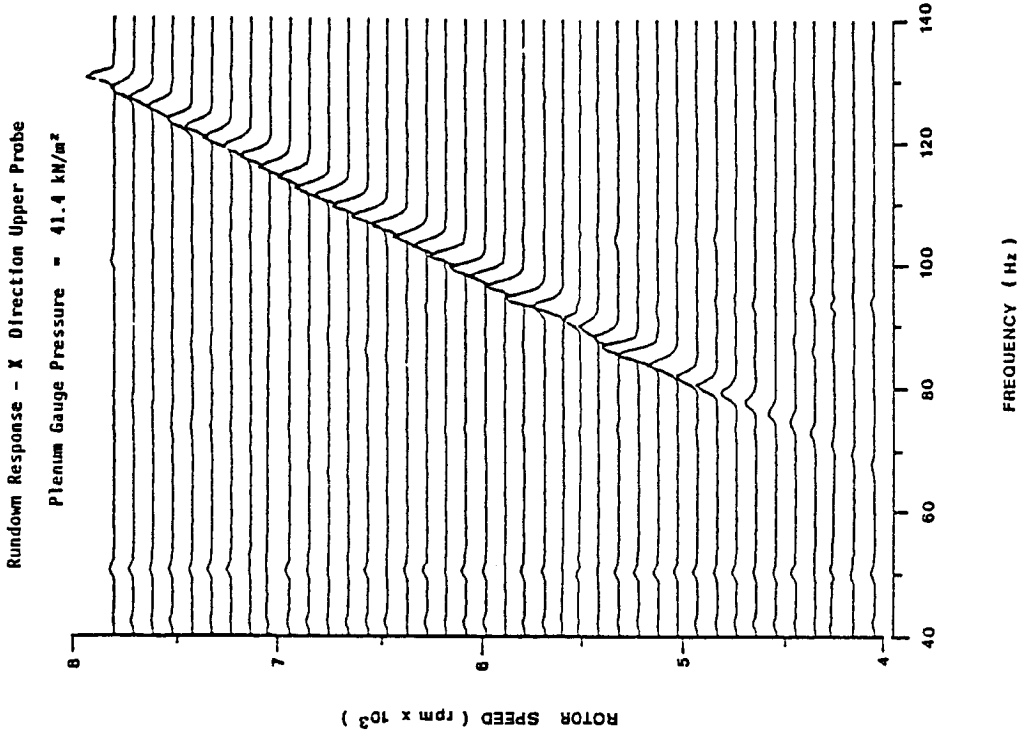
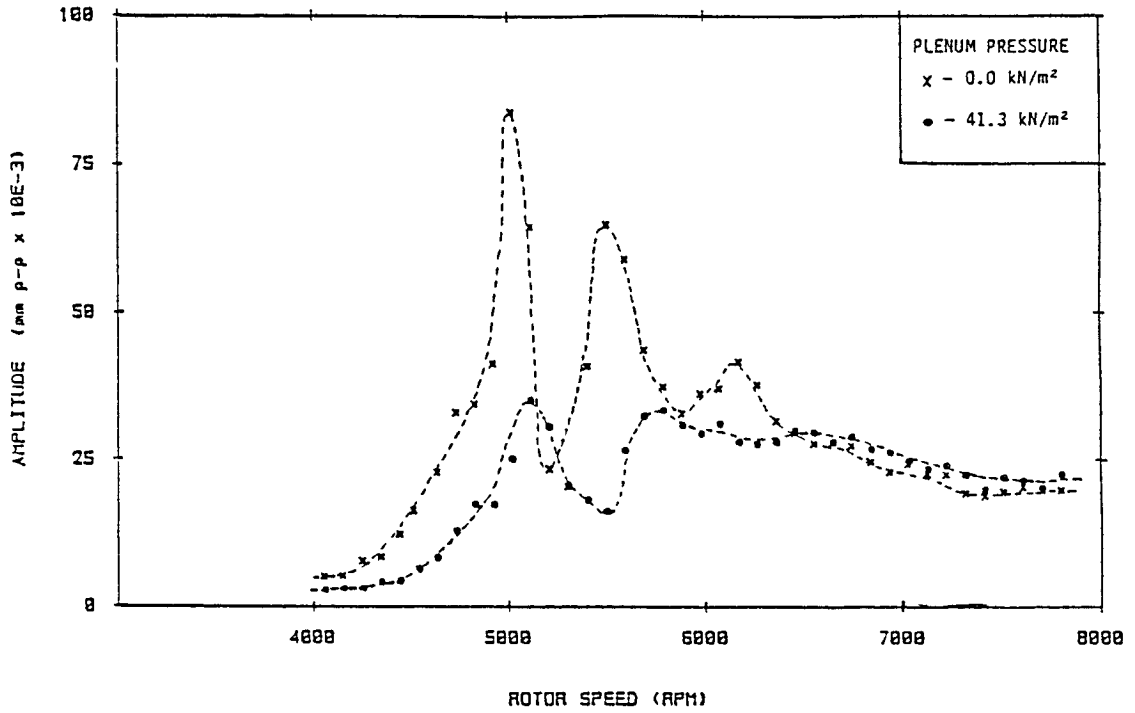


Figure 14 Rundown Response, effect of reverse flow

RUNDOWN RESPONSE - X DIRECTION (Upper Probe)



RUNDOWN RESPONSE - Y DIRECTION (Upper Probe)

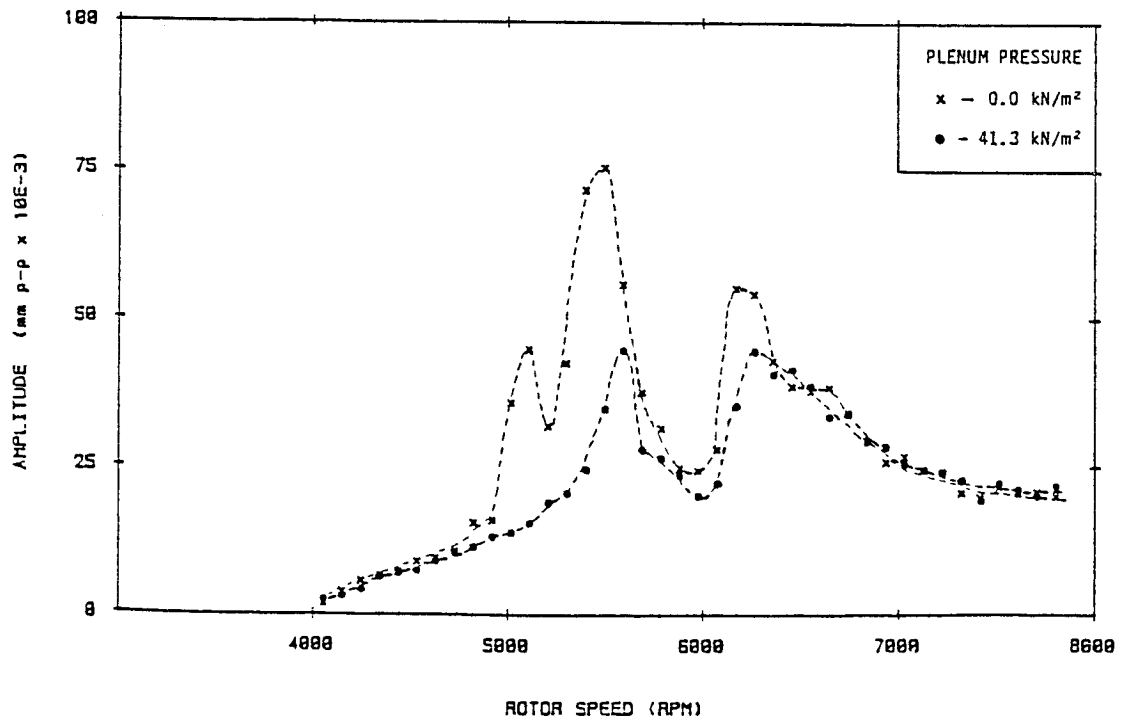


Figure 15 Rundown Response, effect of reverse flow on Synchronous component

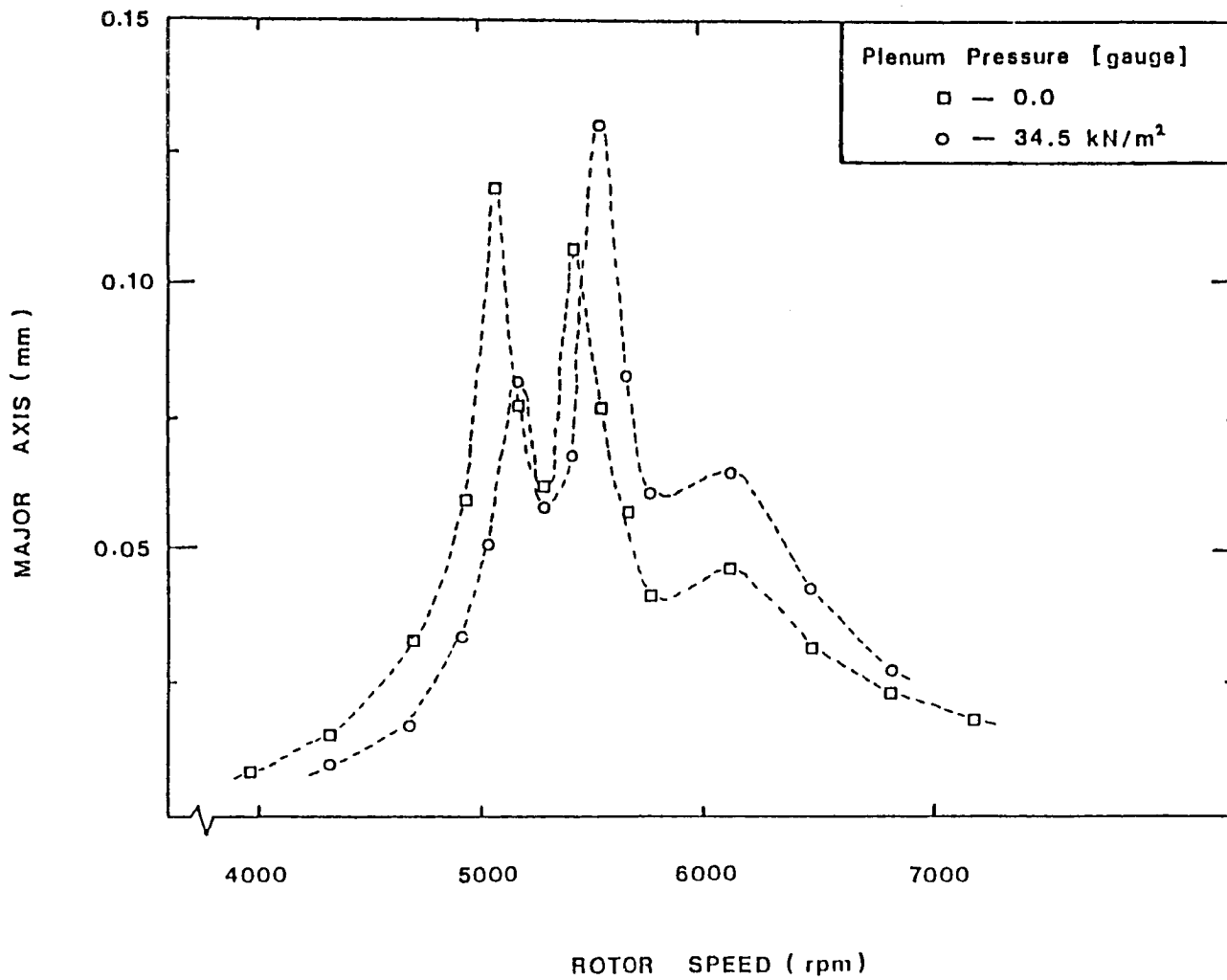


Figure 16 Rotor unbalance response, effect of forward flow

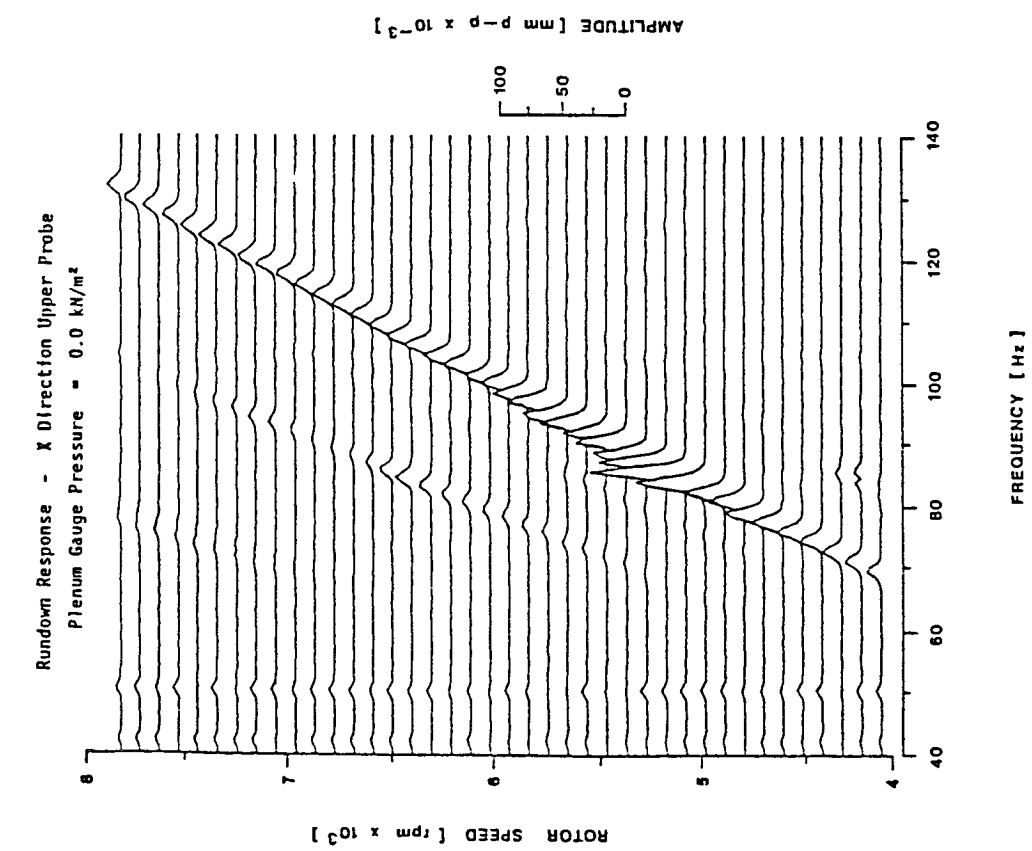
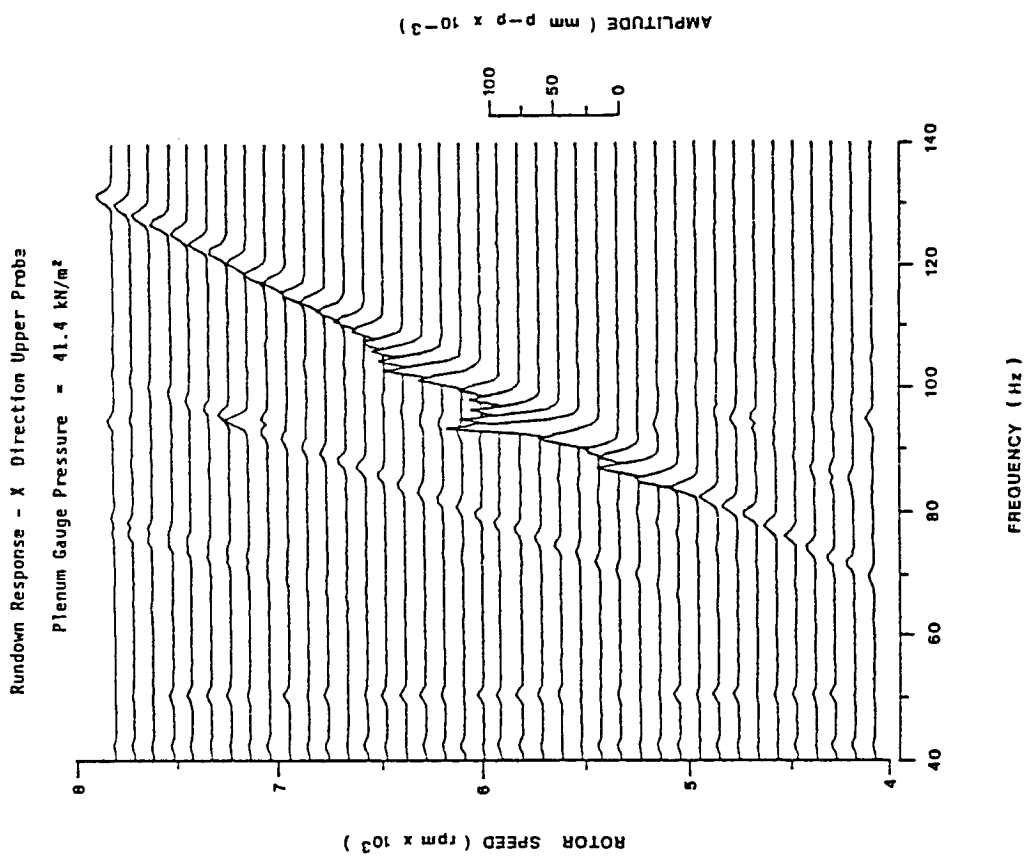


Figure 17 Rundown Response, effect of forward flow

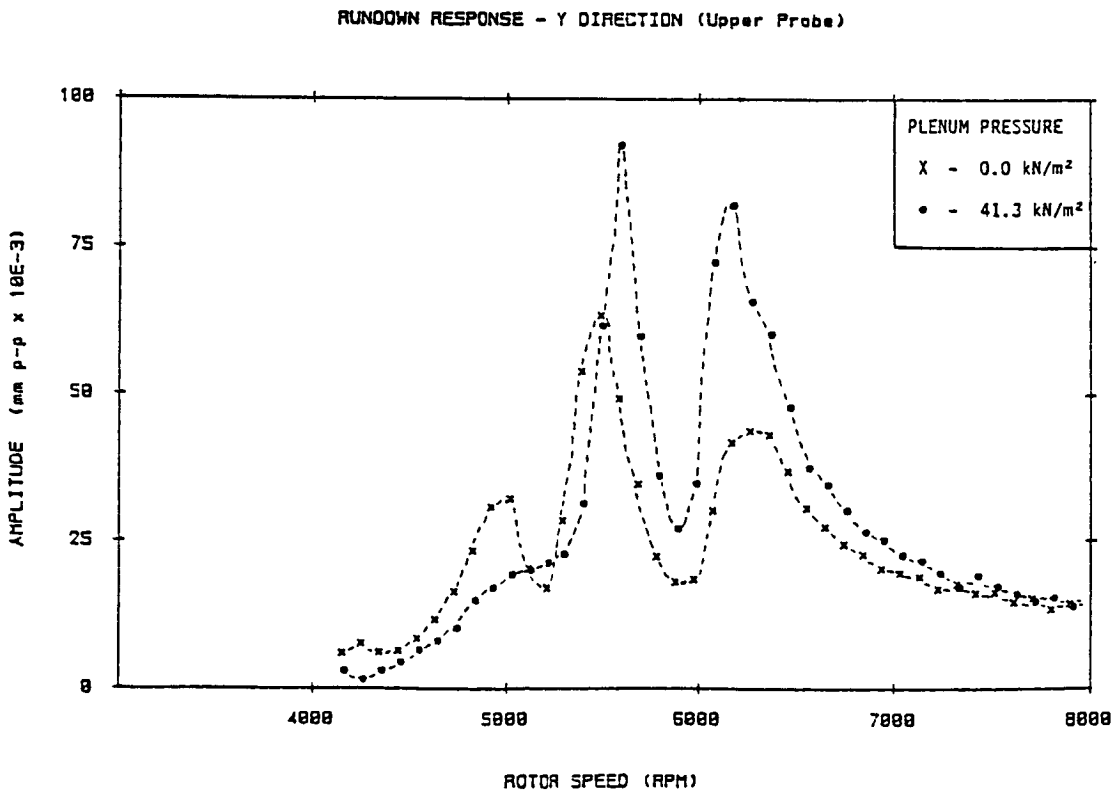
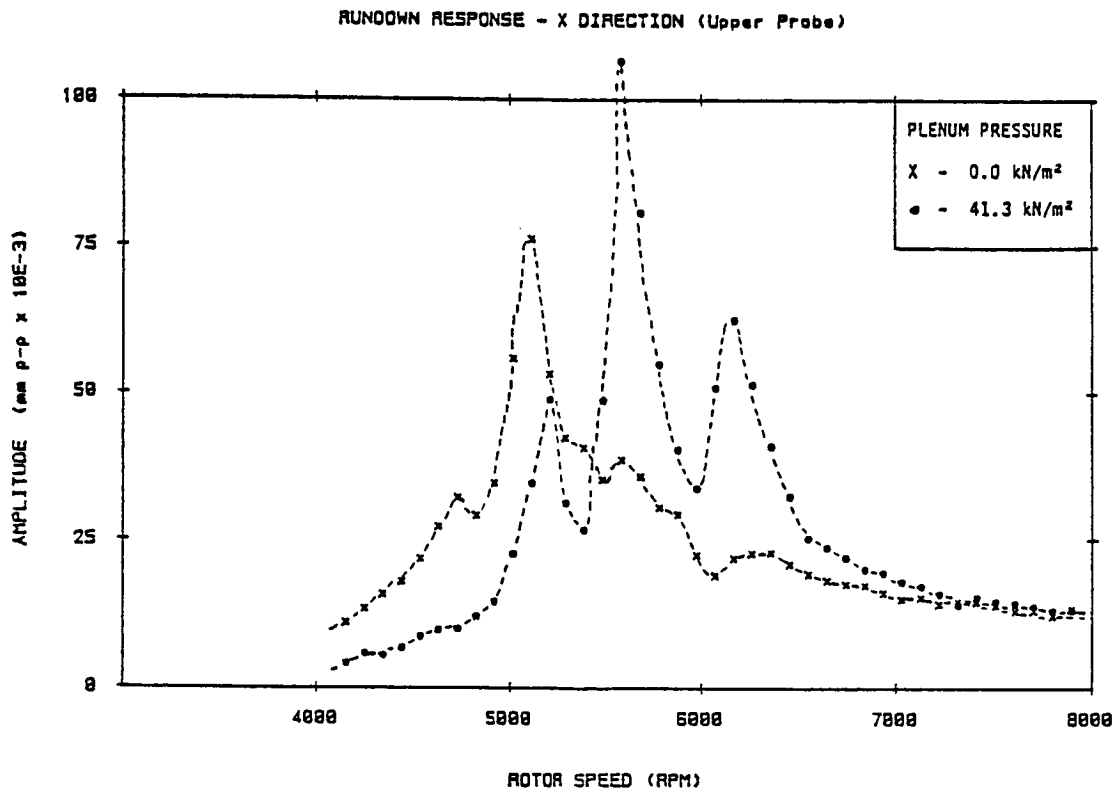


Figure 18    Rundown Response, effect of forward flow on Synchronous component